

UTILIZING THE PYROELECTRIC EFFECT FOR INFRARED HOLOGRAPHIC RECORDING¹

H.A. EGGERT, J. IMBROCK, E. KRÄTZIG

UDC 535.215

© 2004

Universität Osnabrück, Fachbereich Physik
(7, Barbarastrasse, 49069 Osnabrück, Deutschland)

Holographic gratings are stored in photorefractive lithium tantalate crystals with infrared laser pulses without previous sensitization. Through the absorption of infrared light, a thermal grating builds up, which yields a pyroelectric field. Subsequent homogeneous illumination with light of a shorter wavelength excites electrons that drift in the pyroelectric field. Thus, the holographic information of the infrared light pattern is stored as a volume phase hologram that can be read nondestructively. The refractive-index change depends mainly on the absorption coefficient at the wavelength of the recording light and therefore, by choice of suitable dopants, may be extended to telecommunication wavelengths.

to excite electrons even from the shallow traps into the conduction band, the crystals cannot be sensitized for recording via previous illumination with light of a shorter wavelength. Another promising approach to solve this problem uses the pyroelectric effect [8] as a charge driving force. Thermal gradients lead to an electric field via the pyroelectric effect. If the used light intensities are sufficiently high, a contribution to the space charge field caused by the pyroelectric effect has been found in one color experiments [9–11]. But the thermal pattern can also be generated independently from the excitation of electrons. With light of any wavelength at which absorption of the crystal is sufficient, an arbitrary pyroelectric field can be generated. Free electrons, excited with light of another wavelength, compensate for the pyroelectric field and build a space charge field after the thermal pattern has decayed [12].

Introduction

Different methods for holographic recording in photorefractive crystals have been described. Usually, charge carriers are excited by a one-step process and only light of one wavelength is used to record a hologram. Then read-out of information destroys the hologram simultaneously. To overcome this problem, several methods have been developed, e. g., thermal [1], electrical [2], and optical fixing. The latter one can be realized using a two-photon [3] or a two-step process. Two-step processes in lithium niobate (LiNbO₃) [4, 5] and lithium tantalate (LiTaO₃) [6, 7] have been realized using intrinsic defects, namely Nb⁵⁺ at Li site and Ta⁵⁺ at Li site, respectively. Therefore, the crystal has to be sensitized with, e. g., green laser pulses, for the recording of holograms with, e. g., infrared laser pulses. Two-step processes for holographic recording feature two main advantages compared to holographic recording via one-step excitations. Read-out of information with the recording wavelength is nondestructive and the shallow traps populated by sensitization allow recording with infrared light because the required energy to excite electrons into the conduction band is small.

However, the main challenge is holographic recording with one of the wavelengths used in telecommunication. Since the energy of those wavelengths is not sufficient

First we will develop a simplified theory which is suitable to discuss the experimental results. Then we describe the holographic setup and the crystals used. With two interfering infrared recording pulses and one green converting pulse, holograms are stored in stoichiometric and congruent lithium tantalate crystals. The dependences of the refractive-index change and the photoconductivity on the light intensities and on crystal compositions are investigated. Transient refractive-index changes after infrared illumination are also studied. The results are discussed and compared with theory.

1. Theory

1.1. Thermal Gratings

Upon illumination of a crystal with light, temperature changes arise due to absorption. Illumination with a light pattern

$$I(z) = I_0(1 + m \cos Kz) \quad (1)$$

¹This article is dedicated to Professor Marat Soskin on the occasion of his 75th birthday.

leads to a modulated temperature grating [13]. Here, z is a spatial coordinate, m the modulation of the interference pattern and $K = 2\pi/\Lambda$ the absolute value of the grating vector. Upon illumination, the amplitude of the thermal grating grows exponentially,

$$\Delta T(t) = \Delta T_{\text{eff}} m [1 - \exp(-t/\tau_{\text{th}})] \quad (2)$$

with the time constant $\tau_{\text{th}} = \rho c_p \Lambda^2 / (\lambda_t 4\pi^2)$ and the steady state value $\Delta T_{\text{eff}} = \alpha I_0 \Lambda^2 / (\lambda_t 4\pi^2)$. Material parameters for lithium tantalate like density ρ , specific heat c_p , and heat conductivity λ_t are given in Table below. Assuming a grating spacing of $2 \mu\text{m}$, the time constant is $\tau_{\text{th}} = 2.3 \cdot 10^{-7}$ s.

For short pulses ($t_p \ll \tau_{\text{th}}$), the grating amplitude builds up linearly with pulse duration t_p :

$$\Delta T(t_p) = \Delta T^{\text{max}} = m t_p \frac{\alpha I_0}{\rho c_p}. \quad (3)$$

After the end of the pulse, the thermal grating decays exponentially with the same time constant τ_{th} :

$$\Delta T(t) = \Delta T^{\text{max}} \exp[-(t - t_p)/\tau_{\text{th}}]. \quad (4)$$

1.2. Space Charge Field

By means of a temperature gradient, the pyroelectric effect yields an electric field [19]. Together with the above described temperature grating, a modulated electric field arises,

$$E_{\text{pyro}}(z, t) = -\frac{1}{\epsilon \epsilon_0} \frac{\partial P_s}{\partial T} \Delta T(z, t). \quad (5)$$

The electric field builds up and decays with the same time constant τ_{th} as the thermal grating. Assuming short pulse durations, the largest achieved electric field at the end of a pulse is

$$E_{\text{pyro}}^{\text{max}} = -\frac{1}{\epsilon \epsilon_0} \frac{\partial P_s}{\partial T} \Delta T^{\text{max}}. \quad (6)$$

If a homogeneous distribution of electrons is generated in the conduction band within the decay

time of the pyroelectric field, the electrons follow the electric field to compensate it. Thus, a charge pattern is generated. The electrons are recaptured by deep traps and, after complete relaxation of the thermal grating, they build a space charge field.

Upon illumination with an infrared light pattern, no photovoltaic fields are generated without earlier sensitization. Crystals are short-circuited to prevent external fields and as there is only a homogeneous charge carrier distribution, diffusion can be neglected. The arising space charge field depends only on the time difference $\Delta t = t_{532} - t_{1064}$ between the generation of free electrons (start of the green “converting” pulse t_{532}) and the build-up of the temperature grating (start of the infrared “recording” pulse t_{1064}), $E_{\text{s.c}}(\Delta t) = E_{\text{pyro}}(\Delta t)$. If the recording and the converting pulses impinge upon the crystal at the same time, the pyroelectric field builds up linearly, and effectively half of the pyroelectric field contributes to the space charge field

$$E_{\text{s.c}}(\Delta t = 0) = \frac{1}{2} E_{\text{pyro}}^{\text{max}} = -\frac{1}{2} \frac{1}{\epsilon \epsilon_0} \frac{\partial P_s}{\partial T} m t_p \frac{\alpha I_0}{\rho c_p}. \quad (7)$$

The largest space charge field is achieved if the free electrons are generated at the end of the recording pulse ($\Delta t = t_p$). Since the decay of the thermal grating is slow with respect to the pulse duration and to the lifetime of electrons in the conduction band, the grating amplitude can be regarded as constant during the converting pulse duration. Then the pyroelectric field yields a space charge field of

$$E_{\text{s.c}}(\Delta t = t_p) = E_{\text{pyro}}^{\text{max}} = -\frac{1}{\epsilon \epsilon_0} \frac{\partial P_s}{\partial T} m t_p \frac{\alpha I_0}{\rho c_p}. \quad (8)$$

With the parameters for lithium tantalate given in Table, an absorption coefficient of 500 m^{-1} , and typical light intensities of 600 GW/m^2 , we get a space charge field of $E_{\text{s.c}} \approx 320 \text{ kV/m}$.

Depending on photoconductivity of the sample, many pulses (recording and converting) are necessary

The used parameters for congruent lithium tantalate, their meaning, and their values

Symbol	Meaning	Value for LiTaO ₃
λ_t	heat conductivity	1.3 J/(s K m) [14]
ρ	density	7454 kg/m ³ [15]
c_p	specific heat	420 J/(K kg) [16]
α	absorption coefficient	variable
$\partial P_s / \partial T$	pyroelectric coefficient	-176 $\mu\text{C}/(\text{m}^2\text{K})$ [17]
$n_{o,e}$	refractive index for ordinarily (o) and extraordinarily (e) polarized light	2.177, 2.182
$r_{113,333}$	electro-optic coefficient for ordinarily (113) and extraordinarily (333) polarized light (633 nm)	8.4, 30.5 pm/V [18]
ϵ	dielectric coefficient	43.5 [15]
I	light intensity	variable

to build up a space charge field as large as the pyroelectric field. The build up is exponential with the inverse time constant [7, 20]

$$\tau^{-1} = \frac{\sigma_{\text{ph}}}{\epsilon\epsilon_0} = \frac{e\mu}{\epsilon\epsilon_0} \frac{q_{\text{Fe}} S_{\text{Fe}} I_{532} c_{\text{Fe}^{2+}}}{\gamma_{\text{Fe}} c_{\text{Fe}^{2+}}}. \quad (9)$$

Here, $c_{\text{Fe}^{2+}}$ and $c_{\text{Fe}^{3+}}$ are the concentrations of Fe^{2+} and Fe^{3+} , respectively, I_{532} the intensity of the converting light, $q_{\text{Fe}} S_{\text{Fe}}$ the quantum efficiency and absorption cross-section for absorption of a photon and excitation of an electron into the conduction band, and γ_{Fe} the coefficient for recombination of an electron from the conduction band with Fe^{3+} . If the crystal is only illuminated with the converting light, the electrons are redistributed homogeneously and the space charge field is erased exponentially with the same time constant (Eq. 9).

1.3. Refractive-Index Changes

If the crystal is only illuminated with the recording light, the refractive-index changes are transient and decay after the end of the pulse with the time constant τ_{th} . Two effects contribute to these transient changes. The pyroelectric field modulates the refractive-index through the electro-optic effect,

$$\Delta n_{\text{pyro},o,e}(t) = \frac{1}{2} n_{o,e}^3 r_{113,333} \frac{1}{\epsilon\epsilon_0} \frac{\partial P_s}{\partial T} \Delta T(t). \quad (10)$$

Second, the temperature grating leads to a refractive-index change by means of the thermo-optic effect. If the change $\Delta n_{t,o}$ caused by the homogeneous temperature rise is not taken into account, the refractive-index change can be written as

$$\Delta n_{t,o,e}(t) = \frac{\partial n_{o,e}}{\partial T} \Delta T(t). \quad (11)$$

The signs of these contributions are different because the pyroelectric coefficient for lithium tantalate is negative. Assuming a temperature change of 1 K, the refractive-index changes for ordinarily polarized light are $\Delta n_{t,o,o} = 1 \cdot 10^{-5}$ [21] and $\Delta n_{\text{pyro},o} = -1.8 \cdot 10^{-5}$. Therefore, the resulting change is $\Delta n_{\text{res},o} = -0.8 \cdot 10^{-5}$.

If the used crystal is uniaxial, a temperature gradient perpendicular to the c -axis yields no pyroelectric field. Therefore a light pattern with a grating vector perpendicular to the c -axis changes the refractive index only through the thermo-optic effect. The refractive-index change caused by a temperature grating with an amplitude of 1 K for extraordinarily polarized light is $\Delta n_{t,o,e} = 4 \cdot 10^{-5}$.

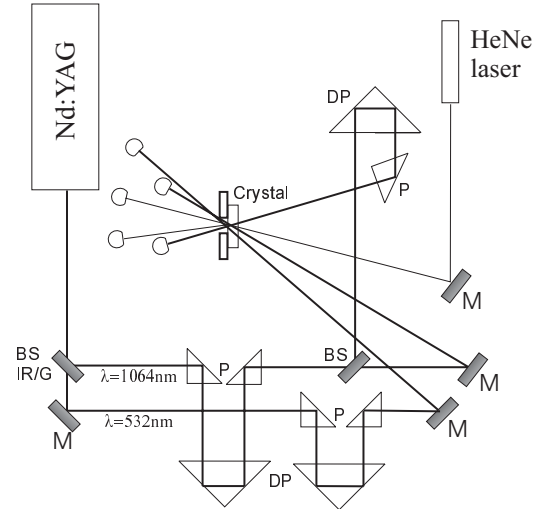


Fig. 1. Schematic drawing of the experimental setup. M – Mirror, BS – Beam-splitter, P – Prism, DP – Double-prism

By illumination of the crystal with recording and converting pulses, the saturation value of the permanent refractive-index change depends on the delay time between the recording and converting pulses:

$$\Delta n_e = -\frac{1}{2} r_{333} n_e^3 E_{s,c}(\Delta t). \quad (12)$$

Thus, a space-charge field of $E_{s,c} \approx 320$ kV/m leads to a refractive-index change for extraordinarily polarized light $\Delta n_e = 5 \cdot 10^{-5}$.

2. Experimental Setup

A schematic drawing of the two-beam setup used in the holographic experiments is given in Fig. 1. A Nd:YAG pulse laser generates infrared ($\lambda = 1064$ nm) pulses of 7 ns length. With a KD*P-crystal, approximately 50 % of the light is frequency doubled to obtain green ($\lambda = 532$ nm) pulses. The intensity of the infrared (recording) pulse can be varied between 80 and 900 GW/m^2 with a $\lambda/2$ -plate and a polarizer. The intensity of the green (converting) pulse can be varied between 150 and 700 GW/m^2 with optical density filters. The grating created by the two intersecting recording pulses has a grating spacing $\Lambda \approx 2 \mu\text{m}$. The recording and converting pulses can be delayed up to 25 ns with respect to each other.

The diffraction efficiency η is monitored with an extraordinarily polarized, Bragg-matched beam of a continuous-wave He–Ne-laser ($\lambda = 633$ nm). With the transmitted I_t and diffracted I_d intensities, the

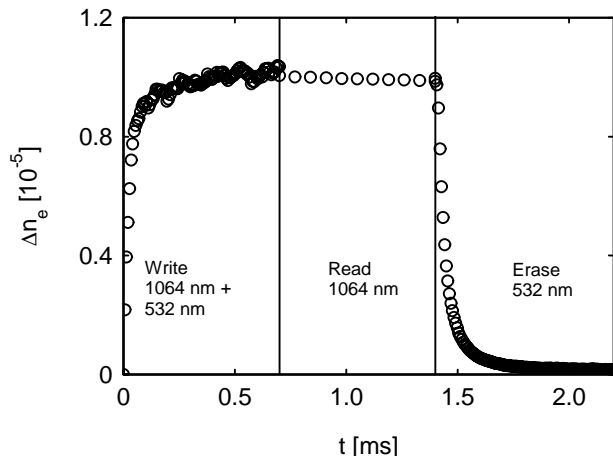


Fig. 2. Refractive-index change Δn_e of a nearly stoichiometric $\text{LiTaO}_3\text{:Fe}$ crystal for a typical write—read—erase cycle. The intensities are $I_{1064} = 730 \text{ GW/m}^2$ and $I_{532} = 700 \text{ GW/m}^2$

diffraction efficiency is $\eta = I_d / (I_t + I_d)$. Using Kogelnik's formula [22]

$$\eta = \sin^2 \left(\frac{\pi d \Delta n}{\lambda \cos \Theta} \right), \quad (13)$$

the refractive-index change can be calculated. Here, d denotes the thickness of the crystal, and Θ is the Bragg angle inside the crystal.

To study the transient effects after illumination of the crystal just with the infrared pulses, a fast Si $p-i-n$ diode is used to monitor the intensity of the diffracted beam of the He—Ne-laser. In order to measure light-induced absorption changes after illumination with the green pulse, the diode can also be used to monitor the intensity of the transmitted beam. The light-induced absorption can be determined according to

$$\alpha_{\text{light}} = 1/d \ln[I(t=0)/I(t)], \quad (14)$$

$I(t=0)$ being the intensity of the transmitted light before and $I(t)$ after the green pulse.

2.1. Crystals

To utilize the pyroelectric charge driving force and to show the difference to other two-step processes, measurements are performed with LiTaO_3 crystals as well of the stoichiometric as of the congruently melting composition. Crystals are doped with iron, since Fe^{2+} ions cause a strong absorption band around 1100 nm due to electron excitation into a real intermediate state [23]. Congruently melting crystals were grown

with the Czochralski-technique and melt-doped with five different concentrations of iron ranging from 100 to 800 wt. ppm Fe. Due to the Li deficit, congruently melting LiTaO_3 crystals contain a large amount of intrinsic defects, namely Ta^{5+} ions on Li site. To decrease the concentration of this antisite, nearly stoichiometric crystals have to be prepared.

To obtain stoichiometric crystals, the lithium concentration of some of the samples is increased with a VTE (vapour—transport—equilibration) treatment. Congruently melting crystals are heated in a Li-rich gas atmosphere at 1380°C until the Li concentration of the gas and of the crystal are in equilibrium [24]. Afterwards, the composition can be determined by measuring the temperature for zero birefringence [25].

The crystals are reduced by annealing in vacuum at temperatures of about 1000°C . This treatment transforms Fe^{3+} into Fe^{2+} ions and therefore increases the absorption at the desired recording wavelength. Absorption coefficients at 1064 nm of the used crystals vary between 100 and 500 m^{-1} . As annealing is performed above the Curie temperature, crystals are poly-domain after cooling down to room temperature. To obtain single-domain crystals, the crystals are heated in an oven above the Curie temperature to $\approx 750^\circ\text{C}$ and an external electric field of about 30 V/cm is applied along the c -axis while cooling down to room temperature.

3. Experimental Results

3.1. Two-color Experiments

If a $\text{LiTaO}_3\text{:Fe}$ crystal of nearly stoichiometric composition is illuminated only with the recording light ($\lambda = 1064 \text{ nm}$), no stationary refractive-index changes are measurable. If a converting pulse ($\lambda = 532 \text{ nm}$) impinges additionally upon the crystal at the same time or some nanoseconds later than the recording pulse, a refractive-index change is achieved. A stored hologram can be read non-destructively with the recording light and erased with the converting light (Fig. 2). In these experiments, a delay time of 9 ns between the arrival of the recording and converting pulses is used. Build up and decay of the refractive-index change can be described by exponential functions.

The dependence of the saturation value of refractive-index change and of photoconductivity on the recording and converting light intensities are investigated. Fig. 3 shows these dependences for variation of the intensity of the recording light. While the saturation value of the refractive-index change increases linearly with intensity,

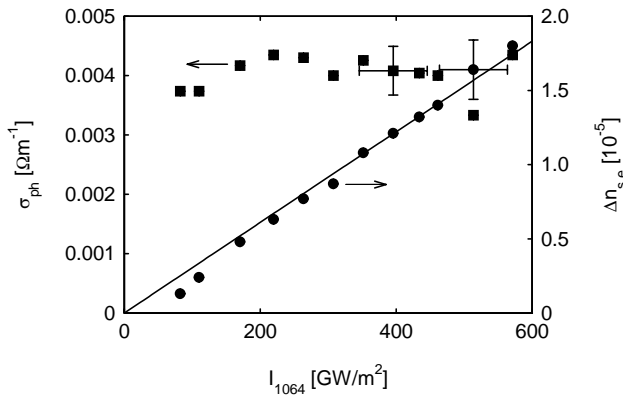


Fig.3. Saturation value of refractive-index change $\Delta n_{s,e}$ (●) and photoconductivity σ (■) of a nearly stoichiometric LiTaO₃:Fe crystal as a function of recording intensity I_{1064} . The intensity of the converting light is $I_{532} = 620$ GW/m². The line is a linear fit to the measured values

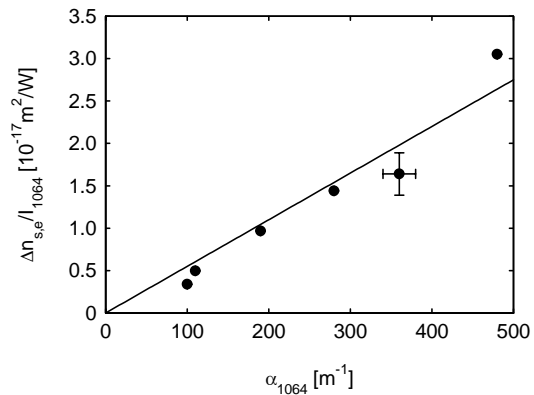


Fig. 5. Saturation value $\Delta n_{s,e}$ of refractive-index change of nearly stoichiometric LiTaO₃:Fe crystals versus absorption coefficient α_{1064} at $\lambda = 1064$ nm. The refractive-index change is normalized to the infrared light intensity I_{1064} . The solid line is a linear fit to the measured data

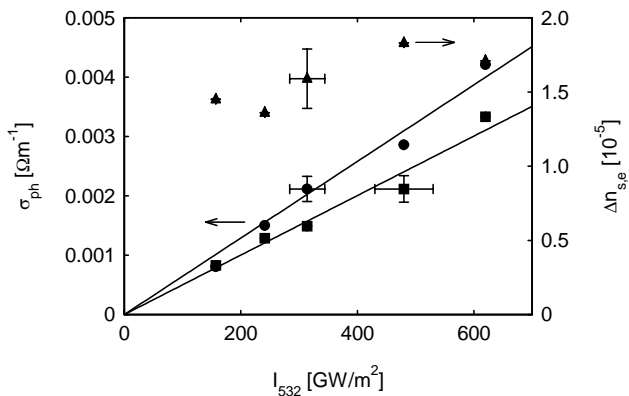


Fig. 4. Saturation value of refractive-index change $\Delta n_{s,e}$ (▲) and photoconductivity σ of a nearly stoichiometric LiTaO₃:Fe crystal for recording (●) and erasing (■) of a hologram as a function of converting intensity I_{532} . The intensity of the recording light is $I_{1064} = 570$ GW/m². The lines are linear fits to the measured values

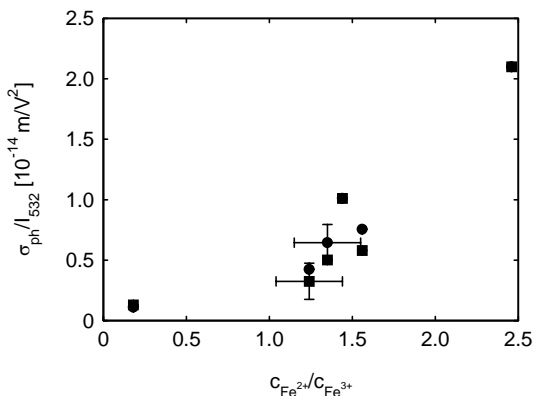


Fig. 6. Photoconductivity σ_{ph} of nearly stoichiometric LiTaO₃:Fe crystals for recording (●) and erasing (■) of a hologram as a function of the $c_{Fe^{2+}}/c_{Fe^{3+}}$ ratio. The photoconductivity has been normalized to the converting intensity I_{532}

the photoconductivity does not depend on the intensity of the recording light. Variation of the converting light intensity yields a linear increase of photoconductivity and nearly no variation of the refractive-index change (Fig. 4). Erasing of a hologram is slightly slower than writing. Additional illumination with infrared pulses during erasure has no influence on the time constant and therefore on the photoconductivity.

Measurements concerning the dependences on dopant concentration and Fe^{2+}/Fe^{3+} concentration ratio are carried out with stoichiometric samples. Some of the used crystals have different iron concentrations,

but there are also crystals from the same boule in different states of annealing. The saturation value of refractive-index change increases linearly with the absorption coefficient α_{1064} at the recording wavelength and therefore with the concentration $c_{Fe^{2+}}$ of filled deep traps (Fig. 5). Since the photoconductivity depends linearly on the intensity of the converting light, the normalized photoconductivity σ/I can be plotted versus the $c_{Fe^{2+}}/c_{Fe^{3+}}$ ratio (Fig. 6). For small concentration ratios, one could see a linear dependence but it seems that a quadratic part arises for higher ratios.

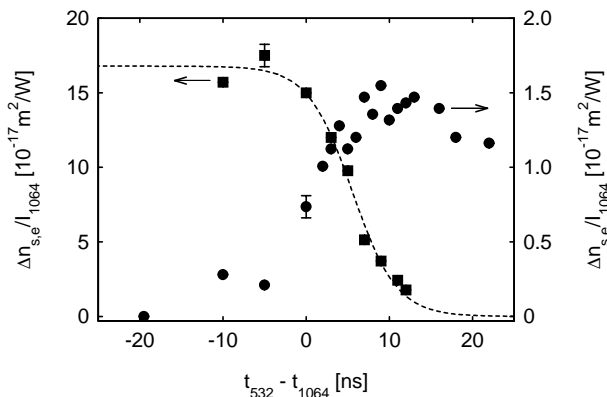


Fig. 7. Saturation value $\Delta n_{s,e}$ of refractive-index change as a function of delay time $t_{532} - t_{1064}$ between the infrared recording pulses and the green converting pulse for a congruent (■, left scale) and a stoichiometric (●, right scale) $\text{LiTaO}_3:\text{Fe}$ crystal. The refractive-index change is normalized to the infrared light intensity I_{1064} . At positive times, the green pulse reaches the crystal after the infrared pulse. The dotted line is a guide to the eye. Please note the different scales for the two crystal compositions

The delay time between the arrival of recording and converting pulses is varied for congruent and stoichiometric crystals. Fig. 7 shows the results. In the congruent sample, the highest refractive-index changes are obtained if the converting pulse reaches the crystal before the recording pulse. If the converting pulse reaches the crystal after the end of the recording pulse, the refractive-index change is only slightly larger than the one obtained in the stoichiometric sample. For this sample, the refractive-index change is at its maximum when the converting pulse reaches the crystal at the end of the recording pulse. If both, the recording and converting pulses, impinge upon the stoichiometric crystal at the same time the value of refractive-index change is approximately half of the maximum change. When the converting pulse reaches the crystal before the recording pulse, the refractive-index change is more than one order of magnitude smaller than for the congruent sample. There is no refractive-index change detectable if the recording pulse impinges upon the crystal after the end of the converting pulse.

3.2. Transient Effects

By illumination of a congruent crystal with one green pulse, absorption changes can be induced. The general results are the same as those published earlier for illumination with ultraviolet pulses [7]. In the

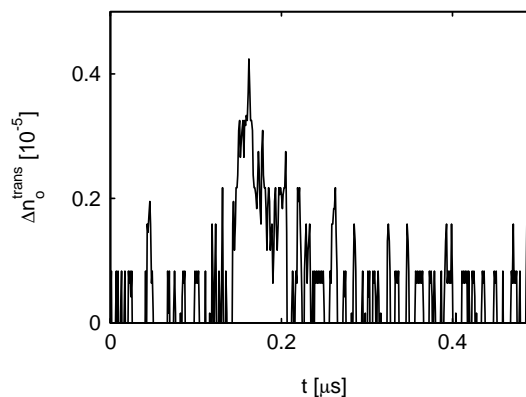


Fig. 8. Refractive-index change $\Delta n_o^{\text{trans}}$ of a congruent $\text{LiTaO}_3:\text{Fe}$ crystal after illumination with one recording pulse as a function of time t . The intensity of the recording pulse is $I_{1064} = 700 \text{ GW/m}^2$. The grating vector of the thermal pattern is parallel to the c -axis of the crystal

stoichiometric crystals, no detectable absorption changes can be induced, i.e., the changes are smaller than $\alpha_{\text{light}} \approx 20 \text{ m}^{-1}$.

If a crystal is illuminated only with the recording light, a transient refractive-index change can be detected (Fig. 8). This measurement has been performed only with a thick congruent sample because the diffraction efficiency of the thin stoichiometric samples was not sufficient to detect a diffracted beam with the Si $p-i-n$ diode. As the change is very small, the signal-to-noise ratio is very poor, but at least the maximum change can be read of as $\Delta n_o = 0.4 \cdot 10^{-5}$ for ordinarily polarized light.

A transient refractive-index change can also be detected if the crystal is illuminated with a light pattern modulated perpendicularly to the c -axis (Fig. 9). The maximum of the refractive-index change is $\Delta n_e = 1.2 \cdot 10^{-5}$ and it decays exponentially with the time constant $\tau \approx 1 \cdot 10^{-7} \text{ s}$.

4. Discussion

The experimental dependences are well described by the theory. Because the half-width of the pulses is 7 ns and the delay time between recording and converting pulses is 9 ns, we can assume that the maximum possible space charge field is achieved [(Eq. 8)]. As Fig. 2 shows, non-destructive read-out of stored holograms

is possible with the recording light. The amplitude of the temperature grating increases linearly with the intensity of the recording light (Eq. 3); this is also valid for the pyroelectric field (Eq. 8) and the saturation value of refractive-index change (Eq. 12, Fig. 3). The converting light only causes a homogeneous temperature rise and thus no spatially modulated pyroelectric field and refractive-index change (Fig. 4) is generated. For a nearly stoichiometric $\text{LiTaO}_3\text{:Fe}$ crystal with an absorption coefficient of $\alpha_{1064} = 480 \text{ m}^{-1}$ at the wavelength of the recording light, a maximum refractive-index change $\Delta n = 2 \cdot 10^{-5}$ is achieved with an recording intensity $I_0 = 570 \text{ GW/m}^2$. According to Eqs. (8) and (12), a refractive-index change $\Delta n = 5 \cdot 10^{-5}$ is estimated. The difference may be due to the decay of the pyroelectric field during the duration of the converting pulse (8). A further reason for the smaller effective field may be lower pyroelectric coefficients in stoichiometric crystals because we use the values for congruent samples in our calculations [26]. Finally, values of the intensities may be uncertain although intensities are averaged over the crystal thickness.

The photoconductivity depends on the concentration of electrons in the conduction band and thus increases linearly with the intensity of the converting light (Eq. 9, Fig. 4). Since it is impossible to excite electrons with the recording light, its intensity has no influence on photoconductivity (Fig. 3). Up to now it is not clear why erasing a hologram is slightly slower than writing.

For hologram recording with one color or with two colors using shallow traps, the saturation value of refractive-index change depends on the concentration $c_{\text{Fe}^{3+}}$ of empty deep traps. In contrast, using the pyroelectric charge driving force, the saturation value of refractive-index change depends on the absorption coefficient at 1064 nm (Eq. 8, Fig. 5) and therefore on the concentration $c_{\text{Fe}^{2+}}$ of filled deep traps. Measurements have been carried out with crystals of different iron concentration and crystals with the same iron concentration but in different states of oxidation confirming that the refractive-index change is achieved utilizing the pyroelectric charge driving force. Similar to one-color recording experiments, the photoconductivity should depend on the $c_{\text{Fe}^{2+}}/c_{\text{Fe}^{3+}}$ ratio (Eq. 9). For small concentration ratios, this dependence seems to be fulfilled (Fig. 6) but, for ratios larger than 1.5, a quadratic dependence seems to be more adequate.

The saturation value of refractive-index change depends also on the delay time between recording and converting pulses (Fig. 7). According to theory, the saturation value of refractive-index change in the

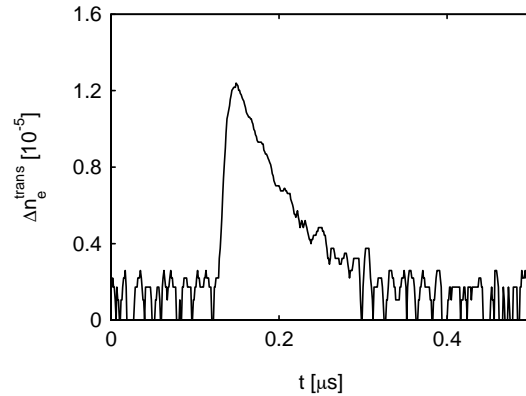


Fig. 9. The same as in Fig. 8 for $\Delta n_e^{\text{trans}}$. The grating vector of the thermal pattern is perpendicular to the c -axis of the crystal

stoichiometric crystal increases by a factor of two between $\Delta t = t_{532} - t_{1064} = 0 \text{ ns}$ and $\Delta t = 9 \text{ ns}$ (Eqs. 7 and 8). Using larger delay times, the saturation value decreases, caused by the decaying pyroelectric field present at the time when the converting pulse impinges upon the crystal. It is possible to record holograms at $\Delta t = -10 \text{ ns}$ indicating that the crystals are nearly stoichiometric. Since the converting pulse arrives entirely before the recording pulse, no pyroelectric charge driving force can arise. The remaining charge driving force is the photovoltaic effect caused by a small amount of populated shallow traps. Earlier experiments under similar conditions yielded a delay time of $\Delta t = -24 \text{ ns}$ for the largest refractive-index changes in congruent lithium tantalate [7]. No refractive-index changes at all can be detected in the stoichiometric samples at delay times less than $\Delta t = -19 \text{ ns}$. Because of that and since no light-induced absorption was detected, we assume that the remaining concentration of shallow traps does not influence the experiments at a delay time of $\Delta t = 9 \text{ ns}$. In the congruent sample, two recording processes are superimposed. If the converting pulse reaches the crystal before the recording pulse, shallow traps are populated and a hologram is recorded using mainly the bulk photovoltaic effect of small polarons as charge driving force. The contribution of the pyroelectric field to the charge driving force increases with delay times between $\Delta t = 0 \text{ ns}$ and $\Delta t = 10 \text{ ns}$. If the converting pulse arrives after the end of the recording pulse, the situation in the congruent crystal is the same as in the stoichiometric one and the only possible charge driving force is the pyroelectric field. At a delay time of $\Delta t = 12 \text{ ns}$, the ratio of the refractive-index changes is $\Delta n_{s,e}(\text{congruent})/\Delta n_{s,e}(\text{stoichiometric}) =$

1.2 with a ratio of the absorption coefficients $\alpha_{1064}(\text{congruent})/\alpha_{1064}(\text{stoichiometric}) = 1.3$. This indicates that the pyroelectric coefficients of congruent and stoichiometric samples differ not too much.

The transient effects after illumination with one recording pulse confirm the presented theory. If a thermal grating with a grating vector parallel to the crystal's c -axis is generated, two different processes contribute to the refractive-index change, the thermo-optic and the pyroelectric via the electro-optic effect (Fig. 8). Experimentally we obtain $\Delta n_o^{\text{exp}} = -0.4 \cdot 10^{-5}$ yielding an amplitude of the temperature grating $\Delta T = 0.5$ K. With an absorption coefficient $\alpha_{1064} = 380 \text{ m}^{-1}$ and an intensity of the recording light $I_{1064} = 700 \text{ GW/m}^2$, the grating amplitude can be calculated as $\Delta T = 0.6$ K (Eq. 3) in good agreement with the above value $\Delta T = 0.5$ K.

If a thermal grating with a grating vector perpendicular to the c -axis is induced, a refractive-index pattern due to the thermo-optic effect arises (Fig. 9). The obtained refractive-index change is $\Delta n_e = 1.2 \cdot 10^{-5}$ which means an amplitude of the temperature grating $\Delta T = 0.3$ K. With Eq. (3), an absorption coefficient for extraordinarily polarized light $\alpha = 190 \text{ m}^{-1}$, and a light intensity $I_{1064} = 796 \text{ GW/m}^2$, the amplitude can be calculated to be $\Delta T = 0.3$ K again in perfect agreement with the above value.

The time constant of the thermal decay can be determined with an exponential fit to the measured data to be $\tau_{\text{th}} \approx 1 \cdot 10^{-7}$ s. The theory has been developed for thick crystals, e.g., the beam waist is small against the crystal thickness. This is not the fact in our experiments, so a heat flow through the crystal surface has to be taken into account. The heat conduction equation has not been solved with this boundary condition, but it seems obvious that it would result in a faster thermal decay and thus smaller time constants. A faster decay of the thermal grating also results in a smaller effective pyroelectric field during the converting pulses duration. This supports the above interpretation that the main reason for the smaller effective field may be the decay of the pyroelectric field during the duration of the converting pulse.

Conclusions

Our experiments show that it is possible to record holograms using the pyroelectric effect as a charge

driving force. This is a promising new method for holographic recording with infrared light and the experimental results can be described well with a simple theory. Since all dependences are known, optimization of holographic recording using this effect should be easy. There are two main advantages: The described method allows the recording of complicated holograms since recording and reading lights have the same wavelength. And the holograms can be read nondestructively. To allow holographic recording at telecommunication wavelengths, the right dopants have to be found. If lithium tantalate is used, iron can provide electrons to compensate for the pyroelectric field. With suitable rare earth elements, the absorption at the desired recording wavelength can be adjusted.

We thank H. Hesse and Ch. Bäumer for the preparation of the stoichiometric lithium tantalate crystals and K. Buse for many helpful discussions.

1. *Amodei J.J., Staebler D.L.*// Appl. Phys. Lett. — 1971. — **18**. — P.540 — 542.
2. *Micheron F., Bismuth G.*// Ibid. — 1973. — **23**. — P.71 — 72.
3. *Von der Linde D., Glass A.M., Rodgers K.F.*// Ibid. — 1974. — **25**. — P.155 — 157.
4. *Buse K., Jermann F., Krätzig E.*// Ferroelectrics. — 1993. — **141**. — P.197 — 205.
5. *Buse K., Jermann F., Krätzig E.*// Appl. Phys. A. — 1994. — **58**. — P.191 — 195.
6. *Vormann H., Krätzig E.*// Solid State Commun. — 1984. — **49**. — P.843 — 847.
7. *Imbrock J., Wevering S., Buse K., Krätzig E.*// J. Opt. Soc. Amer. B. — 1999. — **16**. — P.1392 — 1397.
8. *Vinetskii V.L., Itskovskii M.A.*// Ferroelectrics. — 1978. — **18**. — P.81 — 89.
9. *Buse K.*// J. Opt. Soc. Amer. B. — 1993. — **10**. — P.1266.
10. *Buse K., Pankrath R., Krätzig E.*// Opt. Lett. — 1994. — **19**. — P.260.
11. *Jermann F., Buse K.*// Appl. Phys. B. — 1994. — **59**. — P.437.
12. *Eggert H.A., Imbrock J., Bäumer Ch. et al.*// Opt. Lett. — 2003. — **28**. — P.1975 — 1977.
13. *Eichler H.J., Günter P., Pohl D.W.* Laser-Induced Dynamic Gratings. — Berlin: Springer, 1986.
14. *Lin T.H., Edwards D., Reedy R. E. et al.*// Ferroelectrics. — 1988. — **77**. — P.153 — 160.
15. *Smith R.T., Welsh F. S.*// J. Appl. Phys. — 1971. — **42**. — P.2219 — 2230.
16. *Beerman H. P.*// Infrared Phys. — 1975. — **15**. — P.225 — 231.
17. *Bhalla A.S., Newnham R. E.*// Phys. status solidi (a). — 1980. — **58**. — P.K19 — K24.

18. *Onuki K., Uchida N., Saku T.*// J. Opt. Soc. Amer. — 1972. — **62**. — P.1030 — 1032.
19. *Buse K., Ringhofer K. H.*// Appl. Phys. A. — 1993. — **57**. — P.161.
20. *Kukhtarev N.V., Markov V.B., Odulov S.G. et al.*// Ferroelectrics. — 1979. — **22**. — P.949 — 960.
21. *Abedin K. S., Ito H.*// J. Appl. Phys. — 1996. — **80**. — P.6561 — 6563.
22. *Kogelnik H.*// Bell Syst. Tech. J. — 1969. — **48**. — P.2909 — 2947.
23. *Krätzig E., Orlowski R.*// Appl. Phys. — 1978. — **15**. — P.133 — 139.
24. *Bäumer Ch., David C., Tunyagi A. et al.*// J. Appl. Phys. — 2003. — **93**. — P.3102 — 3104.
25. *Bäumer Ch., Berben D., Buse K. et al.*// Appl. Phys. Lett. — 2003. — **82**. — P.2248 — 2250.
26. *Bartholomäus T., Buse K., Deuper C., Krätzig E.*// Phys. status solidi (a). — 1994. — **142**. — P.K55.

ВИКОРИСТАННЯ ПІРОЕЛЕКТРИЧНОГО ЕФЕКТУ ДЛЯ ІНФРАЧЕРВОНОГО ГОЛОГРАФІЧНОГО ЗАПИСУ

Х. Еггерт, Йо. Імброк, Е. Кретзіг

Резюме

Голографічні ґратки зберігаються в фоторефрактивних кристалах танталату літію при записі лазерними ІЧ-імпульсами без попереднього підвищення чутливості. Завдяки великому поглинанню при ІЧ-освітленні утворюється термічна ґратка, яка спричинює виникнення піроелектричного поля. Подальше однорідне освітлення кристала світлом коротшої довжини хвилі збуджує електрони, які дрейфують в піроелектричному полі. Таким чином голографічна інформація про інфрачервону світлову картину зберігається як об'ємна фазова голограма, що може бути багаторазово зчитана. Зміна показника заломлення залежить в основному від коефіцієнта поглинання на довжині хвилі реєстрації, і добром підходящих домішок вона може бути розширена до довжин хвиль, що застосовуються в телекомунікації.